1995

SELF-SIMILARITY OF THE MEDDY FAMILY IN THE EASTERN NORTH-ATLANTIC

Shapiro, Georgy

OCEANOLOGICA ACTA

Self-similarity of the meddy family in the Eastern North Atlantic

Eddies
Salt lenses
North Atlantic
Temperature and salinity
Modelling

Tourbillons
Lentilles salées
Atlantique Nord
Température et salinité
Modélisation

Georgiy I. SHAPIRO[a], Walter ZENK[b], Sergey L. MESCHANOV[a], Kathy L. SCHULTZ TOKOS [b, c]

[a] P.P. Shirshov Institute of Oceanology, Krasikova Street 23, 117218 Moscow, Russia.

[b] Institut für Meereskunde an der Universität Kiel, Düsternbrooker Weg 20, D 24105 Kiel, Germany.

[c] Present address: 507 Summer Breeze Lane, Sequim, WA 98382, USA.

Received 3/12/93, in revised form 30/6/94, accepted 8/09/94.

ABSTRACT

In this study we analyze two groups of Mediterranean salt lenses: "mid-life" lenses, typically 1-2 years old, observed in the Canary Basin, and younger Meddies from the Iberian Basin. In contrast to turbulent features, vortex lenses have a clear coherent structure in the temperature and salinity fields. This physical property supports the hypothesis that a mathematical description with only a few degrees of freedom may exist. We use nonlinear transformation of variables to find a unique function describing vertical profiles at different locations inside the lens. When this function is found, its existence is considered as "self-similarity" of the lens structure. We also found a common function that describes each group of Meddy, Canary and Iberian, and noted a remarkable difference between the groups. A possible reason for this result might lie in the difference in lens age. Iberian lenses are in a more juvenile state and may go through adjustment transformations before turning into more stable mid-life vortices. The developed parameterization is used to calculate radii and integral heat and salt contents of Meddies.

RÉSUMÉ

Similarités de la famille des meddies dans le nord-est de l'océan Atlantique.

Dans le présent travail, deux groupes de lentilles salées méditerranéennes sont analysés. Des tourbillons en forme de lentilles âgés d'un à deux ans ont été observés dans le bassin des Canaries. Ils se distinguent des meddies plus jeunes du bassin Ibérique. À la différence des formations turbulentes, les lentilles se caractérisent par une nette structure cohérente dans les champs de température et de salinité. Cette propriété justifie une description mathématique avec seulement un petit nombre de degrés de liberté. Nous utilisons la transformation non linéaire des variables pour trouver une fonction décrivant les profils verticaux en différents points à l'intérieur des lentilles. Il en résulte que les structures mathématiques des lentilles analysées sont similaires. Les lentilles plus jeunes du bassin Ibérique peuvent subir encore une transformation pour devenir des tourbillons plus stables, ce qui les distingue des lentilles du bassin des Canaries. La paramétrisation développée est utilisée pour calculer les rayons et les contenus thermique et halin intégrés des meddies.

ZUSAMMENFASSUNG

Ähnlichkeitsbetrachtungen zur Meddy-Familie im östlichen Nordatlantik.

In der vorliegenden Arbeit werden zwei Arten von Salzlinsen aus Mittelmeerwasser (MEDDY) behandelt. Im Kanarenbecken werden linsenförmige Wirbel mit einem Alter von 1-2 Jahren beobachtet. Sie unterscheiden sich von den jüngeren MEDDIES im Iberischen Becken. Im Gegensatz zu Turbulenzelementen sind Linsen durch eine ausgesprochen kohärente Struktur gekennzeichnet. Diese physikalische Eigenschaft erlaubt ihre mathematische Beschreibung mit nur wenigen Freiheitsgraden. Wir verwenden eine nichtlineare Variablentransformation, um eine eindeutige Funktion zur Beschreibung des Vertikalaufbaus von Linsen abzuleiten. Im Ergebnis sind die analysierten Linsenstrukturen in mathematischem Sinne ähnlich. Die jüngeren Linsen im Iberischen Becken können noch einer Anpassungstransformation unterliegen, bevor sie sich in stabilere Wirbel verwandeln, was sie von denjenigen des Kanarenbeckens unterscheidet. Die hier entwickelte Parametrisierung wird zur Berechnung von Durchmessern und der integrierten Wärme- und Salzinhalte von MEDDIES verwendet.

Oceanologica Acta, 1995, **18**, 1, 29-42.

INTRODUCTION

The Mediterranean Water tongue in the northeastern North Atlantic represents the lower boundary of the North Atlantic Central Water. The large-scale distribution of this water mass - an admixture of Gibraltar, Central, and Deep Water - has been well known for many decades. Its spreading and mixing were thought to be rather smooth and uneventful, *i.e.* a well-balanced ratio of advection and diffusion (Defant, 1955) was assumed until the mid-1960s when continuous temperature/salinity profilers became available.

More recently, the detection of drifting and rotating salt lenses (Armi and Zenk, 1984) made a significant reconsideration of the classical concept necessary. Meddies, as the warm and saline submesoscale vortices (McDowell and Rossby, 1978; McWilliams, 1985; Belkin *et al.*, 1986) were subsequently called, definitely play a major role in the mixing at mid-depth in the North Atlantic. They have the ability to conserve their anomalous core-water properties over hundreds of kilometres with only minimal exchange with the surrounding water masses (background fields). Their final decay, potentially years after their generation and triggered by frictional breakdown or by collision with topographic obstacles, represents scattered sources of excess heat and salt preferably in the Canary and the Iberian Basins (Richardson, 1991; Shapiro *et al.*, 1992).

Contemporary Meddy research is no longer only process-oriented. Instead, the interest in Meddies has broadened from the domain of local anomalous properties as seen in biological, chemical, acoustic, and sedimentological parameters to their large-scale effect on deeper water formation and their tomographic impact in relation to observations of the variability of the northeastern Atlantic Ocean.

All the observed salt lenses have a clear coherent structure in the temperature (T) and salinity (S) fields. This means that T and S profiles at different locations in a lens are not absolutely independent. Based on this recognizable physical property, we can assume that a parameterization with only a few degrees of freedom may exist. The ordinary empirical orthogonal functions, which are often used to solve the problem of splitting horizontal and vertical dependencies, would be ineffective in our case because the thickness of a lens varies with radius. A method that seems to be more adequate would permit the deduction of particular T and S profiles by squeezing and/or stretching a reference profile following a prescribed procedure. In the theory of dynamic similarity, structures of that kind are referred to as self-similar ones (Barenblatt, 1982).

Attempts to parameterize the structure of selected lenses have been presented in several papers. It was shown by Shapiro (1986) that the density field in an Arctic lens situated under the ice could be described in self-similar manner. This approach was modified and applied to describe T and S distributions for two well surveyed Meddies in the East Atlantic (Meschanov *et al.*, 1991). Another way was used by Maximenko *et al.* (1988) who proposed a parameterization scheme for a 3-D velocity pattern in the Meddy "Mezopoligon".

The mathematical search for self-similarity in observational data is not simply a formal approach. For example, self-similarity of temperature and salinity profiles in the seasonal thermocline was first found empirically based on a large number of observational data (Miropolskiy *et al.*, 1970) and supported by laboratory modelling (Linden, 1975). It was shown later that this observational result has a strong physical background. The self-similarity is an image (or result) of the stabilization of the governing processes and, in this case, is connected to the asymptotic stage of deepening of the upper mixed layer (Barenblatt, 1982).

The description of a lens with only a few parameters seems to be of practical help, for example, in estimating integral salt and heat content (Armi *et al.*, 1989) of a lens, in calculating disturbances of sound propagation (Lysanov *et al.*, 1989) or in solving acoustic tomography problems.

In this paper we examine the three-dimensional temperature and salinity structure of lenses found in the Canary and the Iberian Basins (Fig.1). The objective is to derive a unique function describing vertical profiles at different positions inside the lenses. If found, we can consider its existence as the mathematical definition of the term, "self-similar structure of a lens". If the same curve describes all the members of a lens group, we refer to this as "group self-similarity".

MATERIALS AND METHODS

The lenses of the same origin have been observed in different environments. As they move from their place of origin, Meddies adjust to the background both dynamically and thermodynamically. The thermodynamic adjustment is controlled by temperature and salinity fluxes between a lens and its surroundings. These fluxes are small and the lens core preserves its *T* and *S* indices for a long time (Armi *et al.*, 1991; Hebert, 1988). The dynamic adjustment is rapid and controlled by background density stratification that differs radically in the Canary and Iberian Basins. It results in changing temperature and salinity profiles because of squeezing or stretching a lens rather than changing *T* and *S* indices of a particular water pieces. The underlying physical mechanism can be explained by the following simple consideration.

Let us consider the lens of radius L, half-thickness h, and density ρ^* located at the interface between two layers of density $\rho^* - \Delta\rho^*$ and $\rho^* + \Delta\rho^*$. Then the scales of azimuthal velocity, lens volume, kinetic and potential energy are $u = g'h/fL$, $V = hL^2$, $E_k = \rho^*_0 u^2 V = \rho^*(g')^2h^3/f^2$, $E_P = \rho^* g'h^2L^2 = \rho^* g'hV$, where f is the Coriolis parameter, $g' = g\Delta\rho^*/\rho^*$ is the reduced gravity acceleration. Full mechanical energy of the lens is $E = E_K + E_P = \rho^* g'hV(1 + Bu)$, where $Bu = g'h^2/(f^2V) = g'h/(fL^2)$ is the Burger number. Assuming mass (ρ^*V) and energy (E) conservation for a lens we can conclude that any increase in background density stratification (g' or $\Delta\rho^*$) results in a decrease in lens thickness.

This is why the anomaly profiles (*i.e.* the difference between profiles in a lens and the background) seem to be more representative than absolute profiles themselves where examination of the self-similarity of a lens structure is concerned. In this paper we use the nonlinear transformation of variables following mainly the model by Shapiro (1986) and the approximation of horizontal parameter distribution following Armi and Zenk (1984).

A lens is assumed to be circular. The distribution of any parameter, preferably temperature and salinity, is written as

$$\Phi(r,z) = \Phi(z) + \Phi'(r,z),$$

where $\Phi(z)$ is the background profile, z is depth, r is radius measured from the lens centre, and $\Phi'(r,z)$ is the anomaly (perturbation) caused by a lens. The main hypothesis that should be examined by processing observational data is that the $\Phi'(r,z)$ distribution could be approximated in a factorized form

$$\Phi'(r,z) = \Phi_M \cdot F(\rho) \cdot B(\xi), \qquad (1)$$

where $\rho = r/L$ is the nondimensional radius, $\xi = (z-z_0)/h(\rho)$ is the nondimensional depth, $h(\rho)$ is a depth scale (see below), L is the total radius of a lens, $B(\xi)$ and $F(\rho)$ are nondimensional functions, $\Phi_M = \Phi'(0,0)$ is the maximum anomaly at the lens centre, $F(0) = 1$, $B(1) = 1$. The key point for the model is that the self-similar profile $B(\xi)$ is a function of ξ only and has no extra dependence on horizontal coordinates.

The vertical depth scale of a lens at a specific radius ρ, $h(\rho)$, characterizes the lens thickness and can be introduced in several different ways. We define it as follows. Let z_1 be the depth where $\Phi'(r,z)$ reaches its maximum value and z_0 be the level in the upper part of a lens, where $\Phi'(r,z)$ changes sign. The value of $h(\rho)$ is defined as the depth interval between z_1 and z_0:

$$h(\rho) = z_1(\rho) - z_0(\rho) \qquad (2)$$

so that $z = z_1$ corresponds to $\xi = 1$ and the maximum value of $B(\xi)$ over ξ equals unity. It is convenient to write $h(\rho)$ as

$$h(\rho) = h_0 \cdot H(\rho) \qquad (2')$$

where $h_0 = h(0)$, $H(\rho)$ is the nondimensional function, $H(0) = 1$.

This definition of z_o (and hence $h(\rho)$) is not obvious but it results in an effective procedure that can be easily formalized for computer processing and is based upon the following basic properties of Meddies.

(i) The vertical gradient of a parameter (*e.g.* salinity, temperature) in the upper part of a lens has an opposite sign compared to background.

(ii) The lowermost open isoline above the lens top is concave.

The existence of the depth level $z = z_0$ where $\Phi'(r,z) = 0$ follows immediately from conditions (i),(ii). Indeed, let us assume that $\partial\Phi/\partial z > 0$ in the lens and $\partial\Phi/\partial z < 0$ in the background water and hence in the area near the lowermost open isoline above the lens top. From (ii) it follows also that in that area $\partial z_\Phi/\partial x > 0$, where $z = z_\Phi(x,y)$ is the equation of the isoline. Using the formula $\partial\Phi/\partial x = -(\partial\Phi/\partial z)\cdot(\partial z_\Phi/\partial x)$ we obtain that $\partial\Phi/\partial x > 0$. It means that $\Phi' = \Phi_L - \Phi_B < 0$, where subscripts L and B stand for "lens" and "background". At the level of maximum Φ we have $\Phi' = \Phi_L - \Phi_B > 0$. Therefore, $\Phi' = 0$ somewhere in between.

From (1)-(2) it follows that the maximum anomaly at any station located in the lens is

$$\max_z[\Phi'(r,z)] = \Phi_m(r) = \Phi_M \cdot F(r) \qquad (3)$$

This model is applied to Meddies found in two regions of the North Atlantic Ocean where lenses were found most frequently: in the Canary and Iberian Basins (Fig.1). Both basins are bounded to the west by the Mid-Atlantic Ridge.

The Canary Basin lies south of the Azores Ridge, separating it from the Iberian Basin off Portugal to the North.

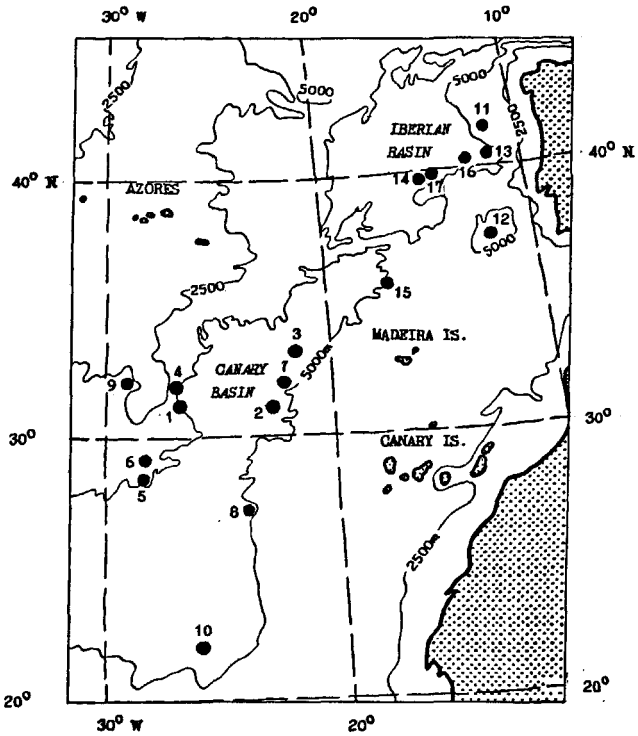

Figure 1

Dots show the locations of Meddies which are marked according to Table 1.

Our most detailed data are available from several Meddies found in the Canary Basin. In this basin, we processed data from nine hydrographic surveys with enhanced spatial resolution which covered seven "mid-life" lenses typically 1-2 years old (Tab. 1). We consider the third survey of lens SHARON (see Tab. 1) together with other Canary lenses, despite its southern location because this lens was first encountered in Canary Basin. In the Iberian Basin we analyzed data of seven "younger" lenses, some of which were still not completely detached from source waters. Lens BIRGIT was found in the southern extent of the Canary Basin but was also included for consideration. Two lenses (VAV-3 and SHARON) were surveyed repeatedly so that we processed 17 surveys in total. The age of each lens was roughly estimated following Armi and Zenk (1984) based on the distance from the probable place of origin (Gulf of Cadiz) and a typical lens velocity of 1-2 miles per day (Käse and Zenk, 1987).

All the measurements except those in lens IRVING were made using a Neil Brown Mark-III CTD profiler. Lens IRVING was measured with a SeaCat SBE-19 CTD profiler. The details of data collection and processing can be found in the original publications referred to in Table 1. For the analysis we used 5- or 4-metre vertically averaged data. Both vertical and horizontal structures were analyzed for the surveys TTO-1, 2, 3, VIT-19, VAV-3 (2), IRVING, SHARON (1, 3), and ANDREAS. The self-similarity of vertical structure was examined for lenses BIRGIT, VAV-3 (1), MET-9, P145A, B, C, D, and MONIKA.

All lenses except SHARON were surveyed over a period of a few days so that one could expect that the lens was not displaced or markedly deformed during the time of the sur-

Table 1

Basic observational parameters of lenses.

#	Lens ID	Coord. of MEDDY center		Date of observ.	NT	NL	Ref.
		Lat., N	Lon., W				
A	TTO-1	31°00'	26°42'	May 81	15	7	AZ
B	TTO-2	31°06'	22°44	June 81	14	6	AZ
C	TTO-3	33°08'	21°33'	June 81	10	3	AZ
D	VIT-19	31°54'	27°00'	June 90	25	16	Be
E	VAV-3(1)	28°21'	28°33'	Mar 89	13	7	MSF
F	VAV-3(2)	29°01'	28°15'	Mar 89	26	12	MSF
G	SHARON(1)	32°00'	22°22'	Sept 84	25	15	AHO
H	SHARON(3)	26°55'	23°37'	Oct 85	28	20	AHO
I	IRVING	32°00'	29°00'	Jan 90	15	14	SME
J	P-145A	36°50'	12°00'	Mar 88	6	1	KBH
K	P-145B	40°30'	12°00'	Mar 88	6	1	KBH
L	P-145C	39°30'	15°00'	Mar 88	6	1	KBH
M	P-145D	35°30'	17°00'	Mar 88	6	1	KBH
N	ANDREAS	40°05'	12°48'	June 89	15	6	HRK
O	MONIKA	39°50'	14°30'	June 89	7	3	HRK
P	MET-9	41°13'	11°30'	Jan 89	7	2	ZMF
Q	BIRGIT	22°00'	26°04'	Nov 86	2	1	ZKS

Abbreviations:
NT - represents the total number of available hydrographic stations occupied in the lens core, lens periphery, and adjacent background waters.
NL - represents the number of stations in a well recognizable lens core that were used to check self-similarity of the vertical lens structure.
AZ - Armi and Zenk (1984), Be - Belkin (pers. comm. 1992), MSF - Maltsev *et al.* (1990), AHO - Armi *et al.* (1989), SME - Shapiro *et al.* (1992), ZKS - Zenk *et al.* (1991), ZMF - Zenk *et al.* (1989), KBH - Käse *et al.* (1989), HRK - Hinrichsen *et al.* (1991).

vey. The validity of this assumption was examined using data of lens VAV-3 which was surveyed twice. The velocity of the lens center was estimated and the relative (referred to the moving lens) locations of the stations were calculated (Meschanov *et al.*, 1991). It was shown that the difference between non-dimensional functions $B(\xi)$, $F(\rho)$, calculated using relative and absolute positions, is small. For SHARON we used values of synchronized radius r which were calculated by Hebert (1988) using a sophisticated synchronization procedure.

The proper identification of a background profile is a crucial point for data processing. Normally, we averaged profiles from several adjacent stations in the background field and from different sides of a lens to exclude perturbations caused by large-scale trends of parameters, internal waves, tidal signals, and development of small-scale structures.

The profiles of temperature and salinity anomalies T'(x,y,z) and S'(x,y,z) were calculated separately for each station in a lens (x,y are coordinates of a station) and local maxima (T_m and S_m) were determined. The profiles at the periphery of a lens usually showed a high degree of fine structure caused probably by intrusions. For the subsequent analysis only those stations were selected that had values of T_m and S_m not less than 25 % of maximum values in the lens centre.

Then the values of z_{0T}, z_{1T}, z_{0S}, z_{1S}, $h_T = z_{1T} - z_{0T}$, $h_S = z_{1S} - z_{0S}$ and stretched vertical coordinates ξ_T and ξ_S were calculated for each anomaly profile according to formula

$$\xi_T = (z - z_{0T})/h_T(x,y) \tag{4}$$

and a similar formula for ξ_S. First we determined the functions $B_T(x,y,\xi_T)$ and $B_S(x,y,\xi_S)$ by

$$B_T(x,y,\xi_T) = T'(x,y,\xi_T)/T_m(x,y) \tag{5}$$

and similarly for salinity.

For each lens the self-similar functions $B_T(\xi_T)$ and $B_S(\xi_S)$ were calculated by averaging $B_T(x,y,\xi_T)$ and $B_S(x,y,\xi_S)$ over stations occupied in the lens core.

According to (3), the horizontal structure function $F_T(\rho)$ was obtained from the distribution of maximum temperature anomaly, $T_m(x,y)$, by nonlinear regression

$$T_m(x,y) = T_M \cdot F_T(\rho) \qquad F_T(\rho) = 1 - \rho^2,$$
$$\rho = \frac{\sqrt{(x - x_T)^2 + (y - y_T)^2}}{L_T}, \tag{6}$$

with four fitting parameters: T_M is the maximum temperature anomaly in the lens centre, L_T is the lens radius estimated from horizontal temperature distribution, x_T, y_T are the coordinates of the lens centre.

The horizontal distribution of the lens thickness $h_T(x,y)$ was approximated by the formula

$$h_T(x,y) = h_{0T} \cdot H_T(\rho), \qquad H_T(\rho) = 1 - \rho^2 \tag{7}$$

where h_{0T} was estimated by linear regression, the value of ρ was given by (6), and parameters x_T, y_T, L_T were taken from the previous step. The same formulas (with subscript S instead of T) were used to describe horizontal salinity distribution.

RESULTS AND DISCUSSION

Figures 2 and 3 show profiles of absolute temperature and salinity, T and S anomalies and nondimensional individual vertical functions $B_T(x,y,\xi_T)$, $B_S(x,y,\xi_S)$ for several selected stations occupied in lenses VIT-19 (Canary Basin) and ANDREAS (Iberian Basin). Nondimensional profiles in stretched variables shown for different stations coincide much better than dimensional profiles. Similar pictures were obtained for other lenses. The self-similar vertical structure functions $B_T(\xi)$ and $B_S(\xi)$ as well as standard deviations are shown in Figs. 4 and 5. For most lenses vertical functions were obtained by averaging individual profiles as described in the previous section. For lenses BIRGIT, P-145A, B, C, D, the vertical functions are based on the only individual profiles in the lens cores because of lack of more data.

For any individual lens (except those having only one station in the lens core) the functions $B_T(x,y,\xi_T)$ and $B_S(x,y,\xi_S)$ depend mostly on the stretched vertical coordinate ξ had a very small dependence on horizontal coordinates x,y, and are close to self-similar profiles $B_T(\xi)$ and $B_S(\xi)$ (Figs. 4, 5). This conclusion proves the existence of a self-similar vertical T,S - structure of lenses. It means that a particular dimensional T (or S) profile at any location in the lens core can be well reconstructed using the self-similar profile B_T (or B_S) and dimensional parameters h_T (or h_S) and T_M (or S_M) and background T,S profiles. The accuracy of this procedure can be estimated from relative values of standard deviation, δB, shown in Figs. 4 and 5. Typically, $\delta B \cong 0.15$ at the level $B = 0.7$. The highest dispersion was found for lens IRVING ($\delta B \cong 0.25$). There are two reasons for this. First, it was really not circular, with the major/minor axes ratio equal to 9/7. Second, the outer core of the lens was damaged by a collision with seamounts, whereas the inner core kept its stable structure (Shapiro *et al.*, 1992). This resulted in perturbation of the lens IRVING.

Generally, different lenses may have different self-similar functions B_T and B_S. Nevertheless, Figs. 4 and 5 (A-I) show a coincidence of nondimensional vertical profiles in the Mediterranean water depth range ($0 < \xi < 2$) between totally different lenses (TTO-1, 2, 3, VIT-19, VAV-3 (1, 2), SHARON-1, 2, IRVING) observed in the Canary Basin. Some peculiarities were found in IRVING. Comparison of two surveys of Meddy "SHARON" separated by one year (Armi *et al.*, 1989) shows some alteration in vertical structure.

The fact that a unique function permits a description of all the members of the group means that there is a "group self-similarity" in vertical structure of the Canary group of Meddy. Figure 6*a* shows "group self-similar functions" B_T and B_S obtained by averaging individual nondimensional profiles for 9 independent surveys carried out in the

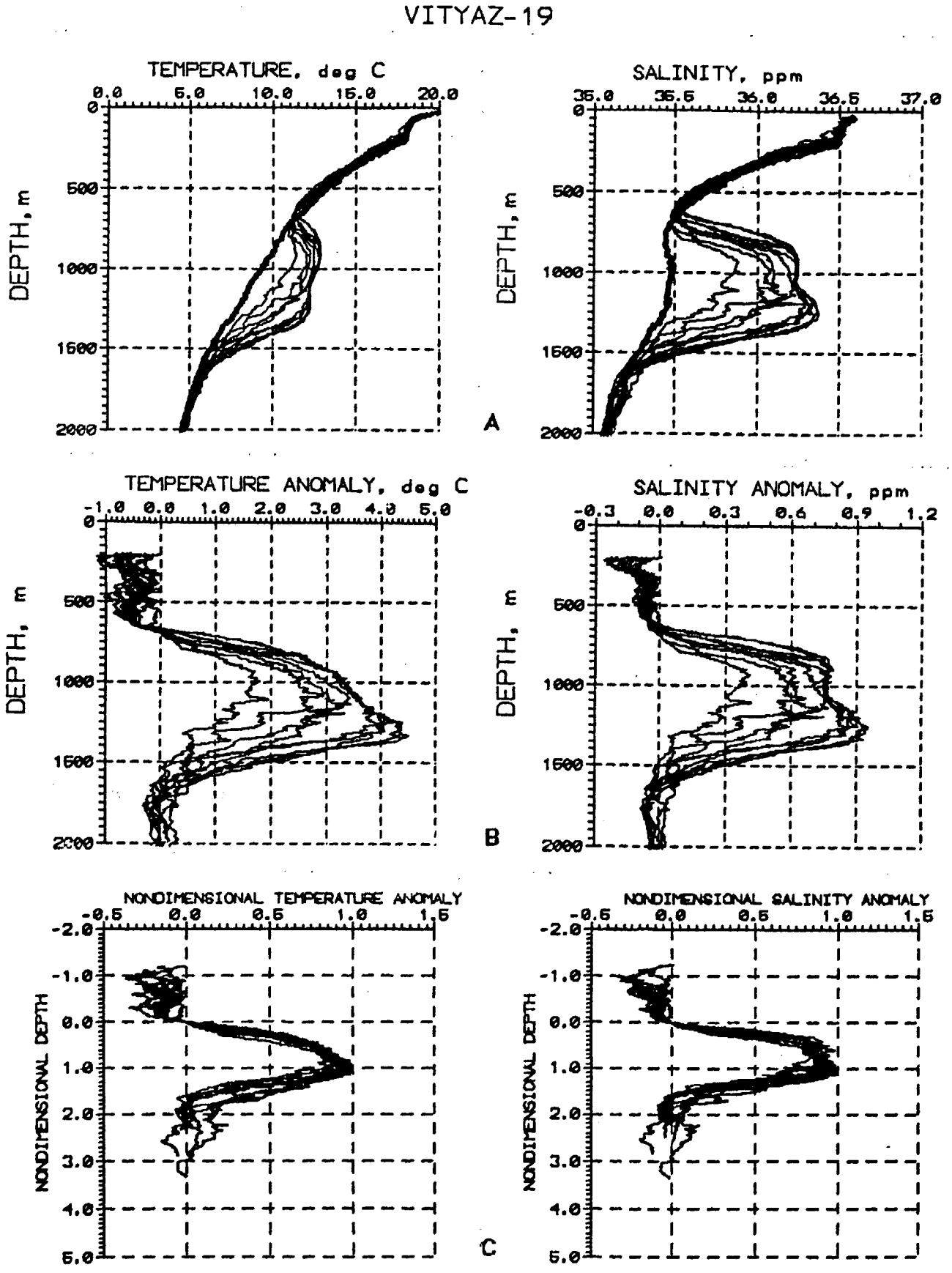

Figure 2

Temperature and salinity profiles at selected stations occupied in Meddy VIT-19 (Canary Basin).
(a) - absolute values
(b) - anomaly compared to background station
(c) - nondimensional profiles in stretched coordinates.

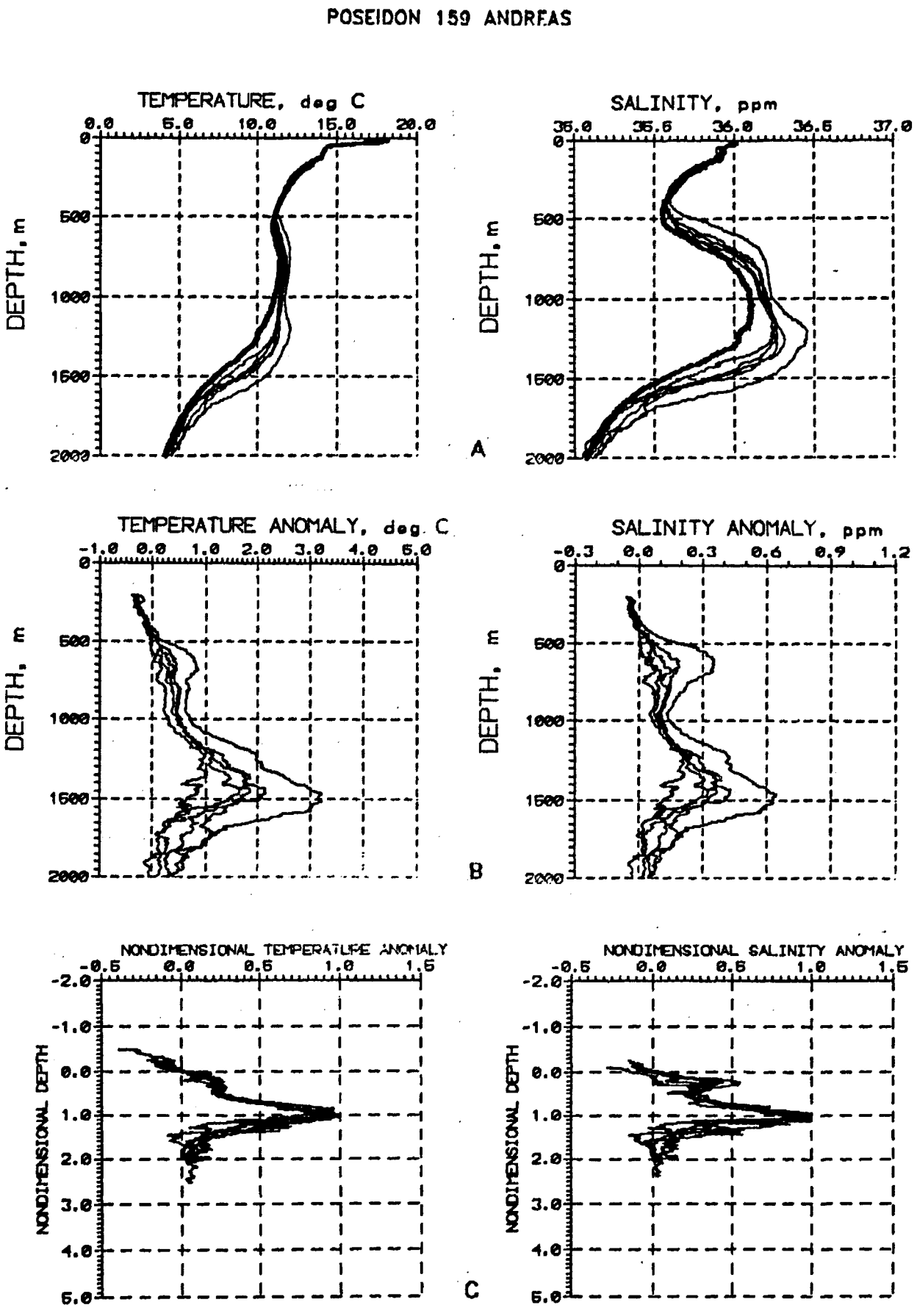

Figure 3

Same as in Fig. 2 for Meddy ANDREAS (Iberian Basin).

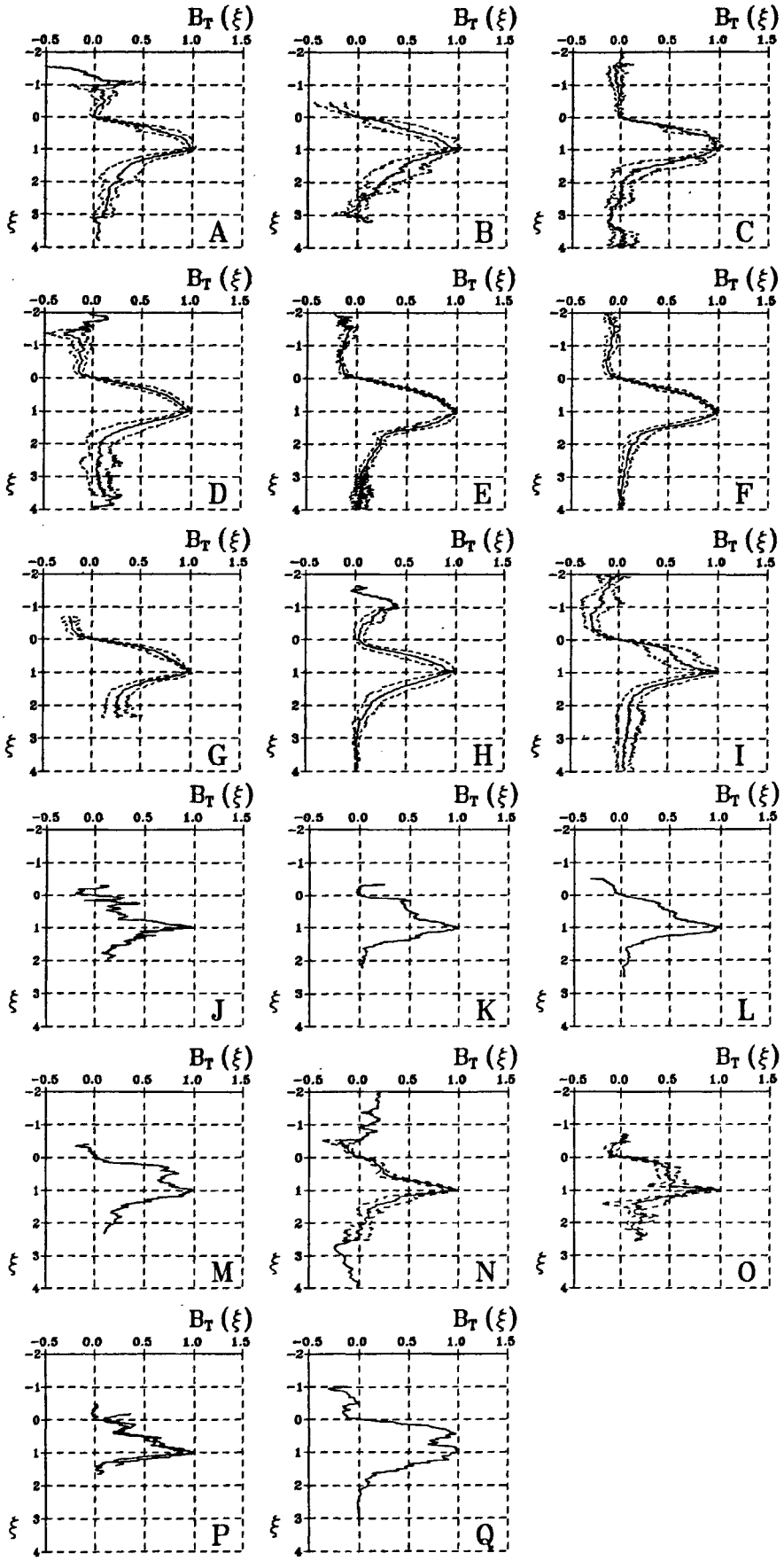

Figure 4

Self-similar temperature vertical functions $B_T(\xi)$. Dashed lines show standard deviations of individual soundings from the mean profile. A-TTO-1, B-TTO-2, C-TTO-3, D-VIT-19, E-VAV-3(1), F-VAV-3(2), G-SHARON(1), H-SHARON(3), I- IRVING, J-P145A, K-P145B, L-P145C, M-P145D, N-ANDREAS, O-MONIKA, P-MET-9, Q-BIRGIT.

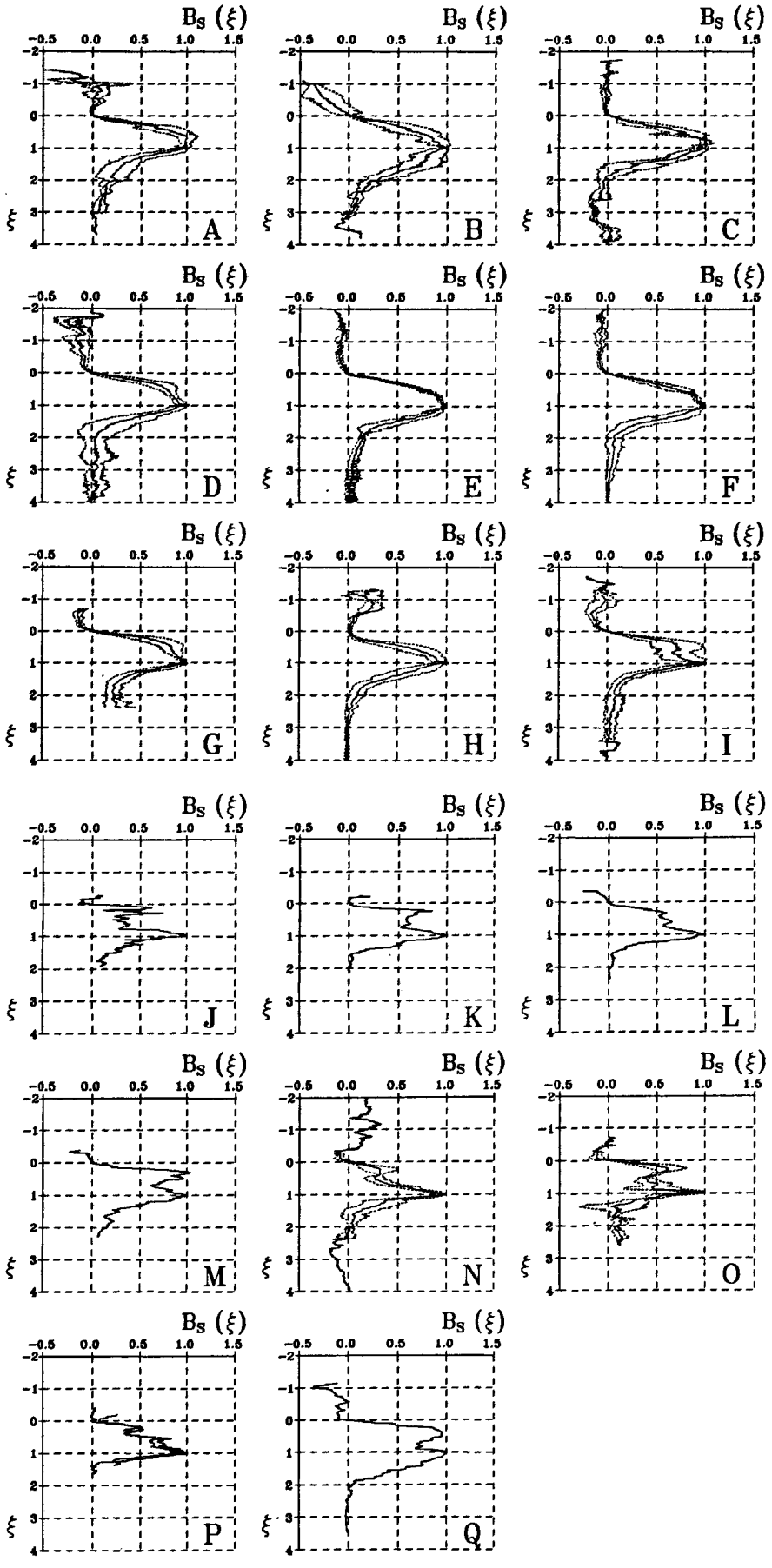

Figure 5

Same as in Fig. 4 for self-similar salinity vertical functions B_S (ξ).

Canary Basin: TTO-1, 2, 3, VIT-19, VAV-3 (1, 2), SHARON-1, 2, IRVING. Outside the lens depth range, the nondimensional vertical profiles are not similar because there is no physical reason to find any coherency there.

Figures 4 and 5 (J-Q) show vertical functions of Iberian lenses. Most of them have only one or two stations occupied in the lens core (P-145A,B,C,D, MET-9). Therefore, the individual self-similarity analysis had to be restricted to lenses ANDREAS and MONIKA. Figures 4 and 5 (N,O) also show that the nondimensional profiles at different locations in lens ANDREAS and MONIKA have approximately the same shape and hence these lenses also have a self-similar vertical structure.

As to "group self-similarity", it was found that various Iberian lenses also have more or less similar vertical structure but that their structure differs markedly from that of Canary lenses. The noses in nondimensional profiles of salinity and temperature anomalies are narrower and sharper than the smooth maxima of Canary lens data. Salinity profiles can have a double maximum (Zenk and Armi, 1990) that is most developed in Meddies P-145A, B, D and MONIKA. Comparing lenses P-145B, MONIKA and P-145D, in the more southern lenses the lower and upper maxima tend to merge and form a wide nose as in Canary lenses. Figure 6*b* shows "group self-similar" vertical profiles for Iberian lenses obtained by averaging data of lenses ANDREAS, MONIKA, P-145A, B, C, D, MET-9. Iberian data are more scattered. This could be explained by more intensive mesoscale dynamic activity in Iberian basin, as recently documented in Lagrangian data off the Portuguese continental slope (Zenk *et al.*, 1992).

The horizontal structure of Canary lenses is shown in Fig. 7*a-d*. A plot of nondimensional temperature and salinity maxima $T_m(x,y)/T_M$ and $S_m(x,y)/S_M$ *versus* nondimensional radius $\rho = r/L$ shows that observational data fit well to the function $F(\rho)$ given by formula (6). Note that both temperature and salinity distributions are well described by the same quadratic parabola (Fig. 7*a,b*). This conclusion is in a good agreement with the results of Armi and Zenk (1984). Figure 7*c,d* shows the horizontal distribution of a lens thickness calculated using temperature ($h_T(\rho)$) and salinity ($h_S(\rho)$) data. The observational data are more scattered than in the case of temperature and salinity maxima (Fig. 7*a,b*) but also reveal a self-similar behaviour in accordance to formula (7).

The main dimensional parameters of self-similarity of Meddies, which have been determined by the procedure described, are listed in Table 2. The difference between L_T

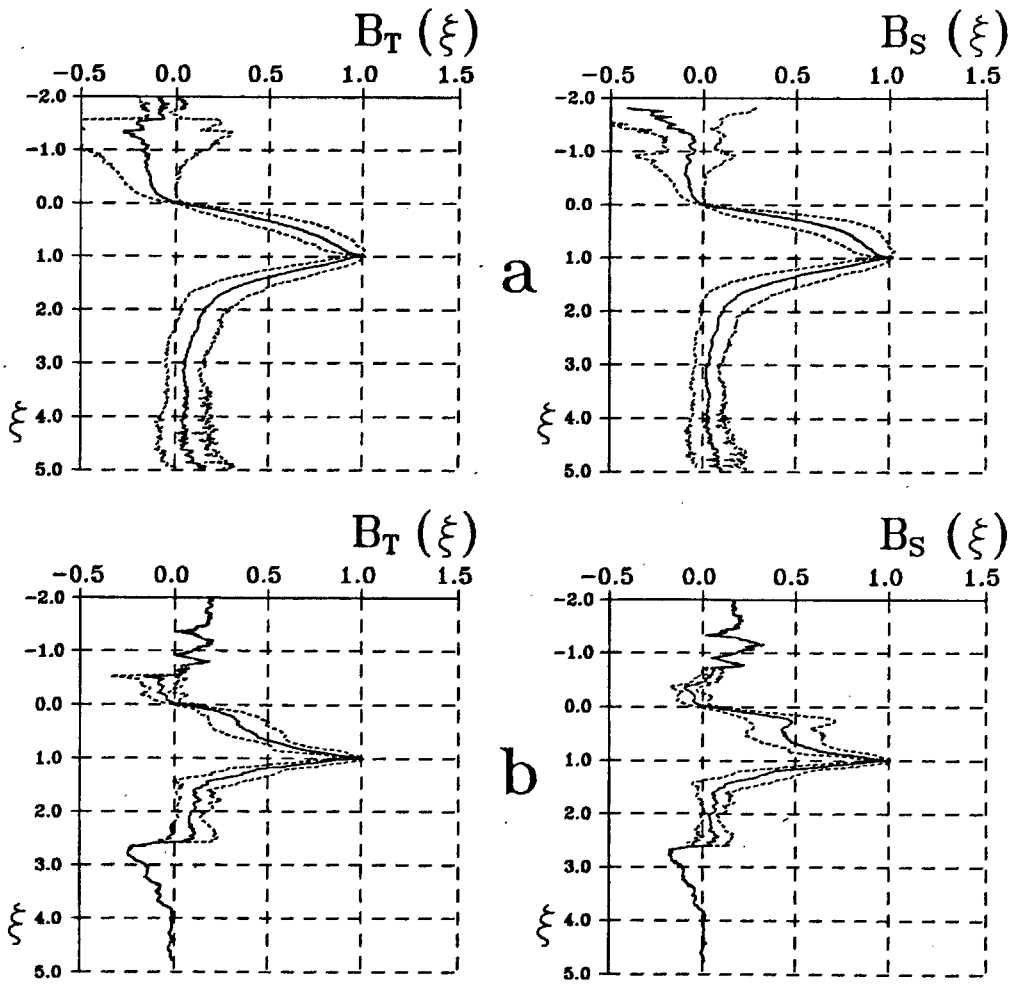

Figure 6

Group self-similar vertical functions for Canary (a) and Iberian (b) Meddies. Dashed lines show the standard deviation of individual profiles.

and L_S is normally less than 5 % so that the value $L_0 = (L_T+L_S)/2$ gives a good approximation for both L_T and L_S. When data did not allow regressional analysis of the horizontal structure to find T_M, S_M, h_{0T} and h_{0S} (marked by stars in Table 2), the corresponding maximum values of individual stations are presented. Standard errors are shown in brackets.

Results of our calculation show that coordinates of lens centre and lens radii calculated using temperature and salinity data are close to each other $x_T \cong x_S \cong x_0$, $y_T \cong y_S \cong y_0$, $L_T \cong L_S \cong L_0$. Hence, the 3-D lens structure is completely described by background profiles and 5 parameters: lens radius, lens thickness in T and S fields, temperature and salinity anomalies in the lens centre.

Lens thickness decreased with increasing distance from the place of origin. This is in qualitative agreement with predictions of theory of frictional lens decay (Shapiro, 1987). According to this theory, intrinsic Ekman layers are formed at the lens border. Ekman pumping generates secondary circulation cells in vertical-radial directions that result in flattening the isopycnal surfaces and decreasing the lens thickness. Another reason for this is the increase of the density stratification in the Canary compared to Iberian Basin (see Section 2).

The above analysis relies on anomalies compared to background and the background profiles change radically between the Iberian and Canary Basins. Are not the major changes in Meddy properties due to different background profiles? To resolve this issue we also analyzed several absolute lens characteristics. No clear dependence of absolute salinity and temperature maxima on the distance from the Strait of Gibraltar or lens latitude was disclosed. Instead, we found a latitudinal dependence of the depths z_{tm} and z_{sm} where absolute maxima were observed. Fig. 8. shows that z_{tm} and z_{sm} do not coincide in the Iberian Basin and tend to be equal at lower latitudes. This fact can be considered as independent evidence of dynamic adjustment of a lens to the background in agreement to the mechanism discussed in Section 2.

The results of the self-similarity analysis are used to estimate integral properties (the total heat and salt excess) of Meddies. In terms of self-similar approximation (1)-(7) the

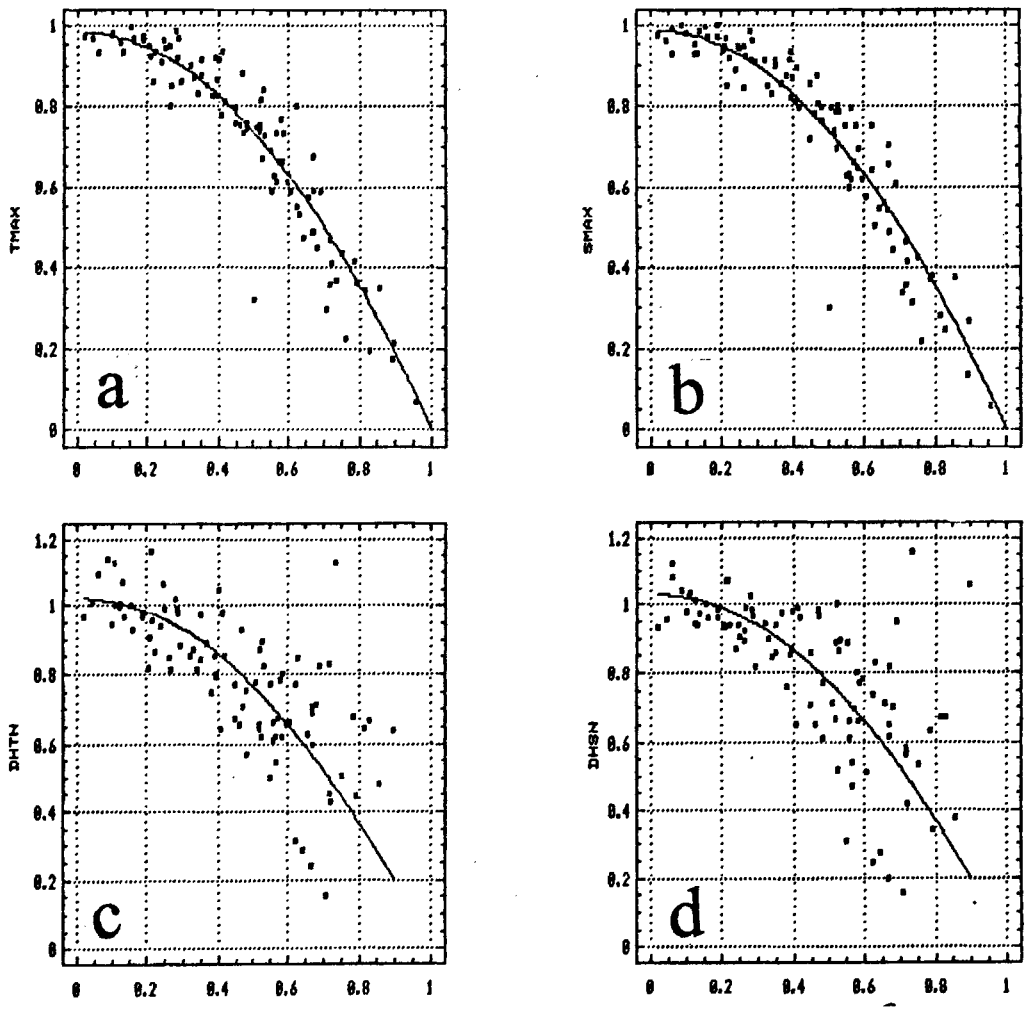

Figure 7

Composed diagram of horizontal distribution of basic lens parameters vs *nondimensional radius =r/L for 8 Canary Meddies.*
(a) - nondimensional temperature Tm/TM maxima (marked by TMAX),
(b) - nondimensional salinity Sm/SM maxima (SMAX),
(c) - nondimensional lens thickness hT/h0T based on temperature data (DHTN),
(d) - nondimensional lens thickness hS/h0S based on salinity data (DHSN).

Table 2

Lens fitting parameters.

#	Lens-ID	T_M (°C)	S_M (p.s.u.)	L_0 (km)	h_{0T} (m)	h_{0S} (m)
A	TTO-1	4.24 (0.16)	0.88 (0.04)	43 (2)	706 (38)	696 (41)
B	TTO-2	3.80 (0.21)	0.82 (0.03)	72 (12)	609 (57)	485 (42)
C	TTO-3	3.10 (0.21)	0.71 (0.04)	40 (2)	497 (77)	522 (70)
D	VIT-19	4.36 (0.10)	0.94 (0.02)	48 (2)	582 (20)	608 (22)
E	VAV-3(1)*	4.53	1.08	–	335	365
F	VAV-3(2)	4.82 (0.06)	1.14 (0.01)	42 (2)	388 (8)	396 (20)
G	SHARON(1)	2.95 (0.05)	0.62 (0.01)	51 (3)	661 (10)	679 (18)
H	SHARON(3)	4.04 (0.13)	0.92 (0.03)	38 (2)	440 (24)	455 (15)
I	IRVING	3.20 (0.13)	0.73 (0.03)	46 (3)	402 (18)	458 (22)
J	P-145A*	2.50	0.58	–	845	845
K	P-145B*	3.35	0.67	–	895	975
L	P-145C*	2.82	0.57	–	765	845
M	P-145D*	2.19	0.42	–	855	865
N	ANDREAS	3.23 (0.05)	0.64 (0.02)	47 (2)	1025 (180)	1120 (200)
O	MONIKA*	1.92	0.38	–	915	965
P	MET-9*	2.12	0.43	–	830	870
Q	BIRGIT*	3.64	0.83	–	450	395

heat (Q) and salt (M) content integrated over the whole lens can be written as

$$Q = 2\pi C_P \int_0^L \int_{z_0}^{z_2} T'(r,z) r dr dz = \frac{\pi}{3} C_P T_M L^2 h_{0T} I_T \quad (8)$$

$$M = 2\pi \int_0^L \int_{z_0}^{z_2} S'(r,z) r dr dz = \frac{\pi}{3} S_M L^2 h_{0S} I_S \quad (9)$$

where

$$I_T = \int_{\xi_0}^{\xi_2} B_T(\xi) d\xi, \qquad I_S = \int_{\xi_0}^{\xi_2} B_S(\xi) d\xi \quad (10)$$

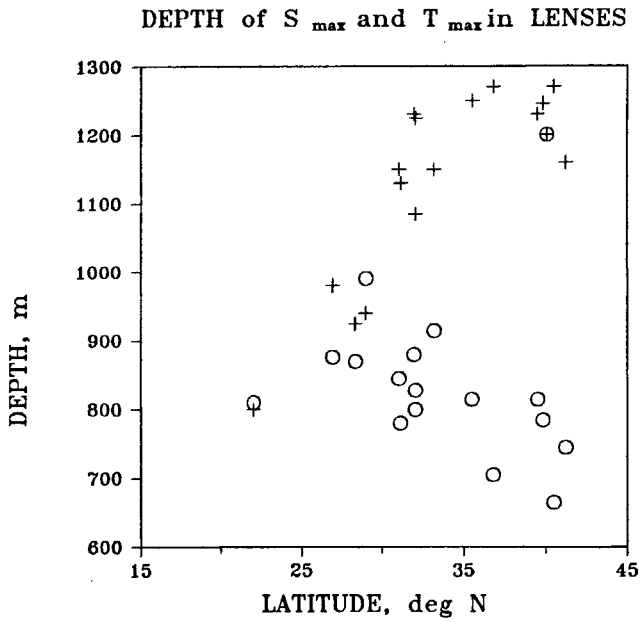

Figure 8

Depths of absolute maxima of temperature (circles) and salinity (crosses) in lenses versus *lens latitude.*

Here C_p is the water heat capacity, z_0, z_2 are the dimensional depths of the upper and lower boundary of the lens, ξ_0, ξ_2 are their nondimensional analogs.

The results of the calculation are presented in Table 3 together with independent estimates (Q_i, M_i) taken from the literature and based on integrating data of individual stations.

In the Canary Basin the values of I_T and I_S estimated using "group average" profiles B_T, B_S are 1.16 and 1.11, respectively. In the Iberian Basin they are 0.79 and 0.76. Comparing I_T and I_S for two surveys of the lens VAV-3, the discrepancy is less than 10 % ; this value can be considered as the estimation of accuracy of data presented in Table 3. In the Iberian Basin the values of I_T and I_S are systematically lower than in the Canary Basin in agreement with the difference in self-similar profiles for the two groups. The southernmost and hence the oldest of Iberian lenses, P-145D, has the highest values of I_T and I_S that are close to typical values of Canary lenses. This supports the idea that the transformation of a lens vertical structure correlates to its age.

CONCLUSION

In this study we concentrated mostly on "mid-life" lenses, typically 1-2 years old, found in the Canary Basin, and on younger lenses from the Iberian Basin. Using a nonlinear transformation of variables we found that for all Mediterranean lenses analyzed there exists a unique nondimensional curve describing vertical profiles at different positions inside the lens. Its existence is the mathematical demonstration of the self- similarity of the Meddy's vertical structure. We processed data from nine surveys in the Canary Basin and seven surveys in the Iberian Basin and found that this conclusion is valid for both Canary and Iberian lenses. We

Table 3

Integral properties of meddies.

#	Lens-ID	I_T	I_S	Q 10^{19} J	M 10^{12} kg	Q_i 10^{19} J	M_i 10^{12} kg	Ref.
A	TTO-1	1.27	1.24	3.09	1.47	–	–	–
B	TTO-2	1.18	1.39	6.28	3.03	–	–	–
C	TTO-3	1.08	1.04	1.15	0.64	–	–	–
D	VIT-19	1.26	1.12	3.34	1.59	–	–	–
E	VAV-3(1)	1.33	1.24	–	–	–	–	–
F	VAV-3(2)	1.21	1.16	1.81	1.00	1.78	0.91	MSS
G	SHARON(1)	1.24	1.23	2.86	1.43	2.52	1.78	He
H	SHARON(3)	1.02	0.95	1.17	0.62	0.68	0.59	He
I	IRVING	1.03	0.93	1.23	0.69	1.31	0.72	SME
J	P-145A	0.65	0.73	–	–	–	–	–
K	P-145B	0.84	0.84	–	–	–	–	–
L	P-145C	0.84	0.79	–	–	–	–	–
M	P-145D	1.09	1.11	–	–	–	–	–
N	ANDREAS	0.65	0.64	2.16	1.10	–	–	–
O	MONIKA	0.88	0.76	–	–	–	–	–
P	MET-9	0.68	0.72	–	–	–	–	–
Q	BIRGIT	1.21	1.29	–	–	–	–	–

Abbreviations:
MSS - Meschanov *et al.* (1991), He - Hebert (1988), SME - Shapiro *et al.* (1992).

found also that the horizontal structure of different Meddies is described by a unique nondimensional function.

According to their vertical structure, the Meddies can be subdivided into two groups, one containing Canary lenses and the other containing Iberian lenses. The results show a good coincidence (*i.e.* "group self-similarity") in nondimensional profiles between different lenses from each group, Canary and Iberian, of Meddy family separately. Based on anomaly analysis, we found a remarkable difference between the two groups in both integral and differential properties. Analyzing absolute lens characteristics we found no spatial trend in salinity and temperature maxima whereas there was a clear latitudinal dependence of the depths where these maxima were observed.

A possible reason for the difference between lenses from the Canary and Iberian Basins is the difference in their age. Iberian lenses are in a more juvenile state and may go through adjustment transformations before turning into more stable, mid-life vortices as found in the Canary Basin. The temperature and salinity indices in a lens core are mainly preserved whereas vertical distribution of parameters changes while a lens moves from the place of origin.

Acknowledgements

This work was partially carried out during the visit of G. Shapiro to the Institut für Meereskunde (Kiel). The investigation was financially supported by Deutsche Forschungsgemeinschaft (SFB 133) and the Russian Fund for Fundamental Research (grants # 93-05-14006, 94-05-17302a). We are grateful to the anonymous reviewers for their comments.

REFERENCES

Armi L., W. Zenk (1984). Large lenses of highly saline Mediterranean Water. *Journal of Physical Oceanography* **14**, 1560-1576.

Armi L., D. Hebert, N. Oakey, J.F. Price, P.L. Richardson, H.T. Rossby (1989). Two years in the life of Mediterranean salt lens. *Journal of Physical Oceanography* **19**, 354-370.

Barenblatt G.I. (1982). *Similarity, Self-Similarity, and Intermediate Asymptotics*. Leningrad, Gidrometeizdat, 255 p. (in Russian).

Belkin I.M., M.V. Emelianov, A.G. Kostianoy, K.N. Fedorov (1986). Thermohaline structure of intermediate waters of the ocean and intrathermocline eddies. In: *Intrathermocline eddies in the ocean*. Moscow, IOAN, 8-34 (in Russian).

Defant A. (1955). Die Ausbreitung des Mittelmeerwassers im Nordatlantischen Ozean. *Pap. Mar. Biolog. Oceanogr.* **1**, 465-470.

Hebert D.L. (1988). *A Mediterranean salt lens*. Ph.D. Thesis. Dalhousie University, Halifax, Nova Scotia, 187 p.

Hinrichsen H.-H., M. Rhein, R.H. Käse, W. Zenk (1993). Mediterranean water tongue and its chlorofluoromethanes signal in the Iberian Basin in early summer 1989, *Journal of Geophysical Research* **98**, 8405-8412.

Käse R.H., W. Zenk (1987). Reconstructed Mediterranean salt lenses trajectories. *Journal of Physical Oceanography* **17**, 158-163.

Käse R.H., A. Beckmann, H.-H. Hinrichsen (1989). Observational evidence of salt lens formation in the Iberian Basin. *Journal of Geophysical Research* **94**, 4905-4912.

Linden P.F. (1975). The deepening of a mixed layer in a stratified fluid. *Journal of Fluid Mechanics* **71**, 385-405.

Lysanov Yu.P., A.M. Plotkin, G.I. Shapiro (1989). The effect of intrathermocline lenses on acoustic fields in the ocean. *Izvestija Akademii Nauk SSSR. Fizika atmosfery i okeana* **25**, 1272-1280 (in Russian).

Maltsev N.E., K.D. Sabinin, A.V. Furduev (1990). An acoustic-oceanologic experiment at the lens of Mediterranean waters in the Atlantic Ocean. *Akusticheskij Zhurnal* **36**, 86-93 (in Russian).

Maximenko N.A. (1988). Comparative analysis of currents and density fields in a Mediterranean lens according "MESOPOLIGON" data, In: *Gidrofizicheskie issledovaniya po programme MESOPOLIGON*, Moscow, Nauka, 69-75 (in Russian).

McDowell S.E., H.T. Rossby (1978). Mediterranean Water: An intensive mesoscale eddy off the Bahamas. *Science* **202**, 1085-1087.

McWilliams J.C. (1985). Submesoscale, coherent vortices in the ocean. *Reviews of Geophysics* **23**, 165-182.

Meschanov S.L., G.I. Shapiro, S.M. Shapovalov (1991). Self-similarity of temperature and salinity distribution in Mediterranean lenses. In: *Vortex lenses and eddies in the Northeast Atlantic*. Moscow, IOAN, 111-120 (in Russian).

Miropolskiy Yu.Z., B.N. Filushkin, P.P. Chernyshkov (1970). On parametric description of temperature profiles in active layer of the ocean. *Okeanologia* **10**, 1101-1107 (in Russian).

Richardson P.L., M.S. McCartney, C. Maillard (1991). A search for meddies in historical data. *Dynamics of Atmospheres and Oceans* **15**, 241-265.

Shapiro G.I. (1986). On some properties of vortex lenses in continuously stratified ocean. In: *Intrathermocline eddies in the ocean*, Moscow, IOAN, 79-85 (in Russian).

Shapiro G.I. (1987). To the theory of quasigeostrophic motions of finite amplitude in the viscous stratified ocean. *Okeanologia* **31**, 18-24 (in Russian).

Shapiro G.I., S.L. Meschanov, M.V. Emelianov (1992). Mediterranean lens after collision with seamounts, *Okeanologia* **32**, 420-427 (in Russian).

Zenk W., L. Armi (1990). The complex spreading pattern of Mediterranean Water off the Portuguese continental slope. *Deep-Sea Research* **37**, 1805-1833.

Zenk W., B. Klein, M. Schröder (1991). Cape Verde Frontal Zone. *Deep-Sea Research* **38**, Suppl.1, 505-530.

Zenk W., T.J. Müller, G. Wefer (1989). BARLAVENTO- Expedition, Reise Nr.9, 29 Dezember 1988 - 17 März 1989. *Meteor- Berichte*, Universität Hamburg, **89**-2, 238.

Zenk W., K. Schultz Tokos, O. Boebel (1992). New Observation of Meddy movement south of the Tejo Plateau, *Geophysical Research Letters* **19**, 2389-2392.